Optical absorption in the substituted phenylene-based conjugated polymers: Theory and experiment

M. Chandross*
Department of Physics, University of Arizona, Tucson, Arizona 85721

S. Mazumdar
Department of Physics and The Optical Sciences Center, University of Arizona, Tucson, Arizona 85721

M. Liess, P. A. Lane, and Z. V. Vardeny
Department of Physics, University of Utah, Salt Lake City, Utah 84112

M. Hamaguchi and K. Yoshino
Department of Electronic Engineering, Faculty of Engineering, Osaka University, 2-1 Yamada-Oka, Suita, Osaka 565, Japan
(Received 25 September 1995; revised manuscript received 22 May 1996)

We investigate theoretically and experimentally the effects of (2,5) chemical substitution on the optical absorption in the phenylene-based conjugated polymers. Theoretically, substitution destroys both the charge-conjugation symmetry and spatial symmetry that characterize the unsubstituted materials. Within Coulomb-correlated theoretical models, the effect of broken charge-conjugation symmetry alone on the underlying electronic structure and on the absorption spectrum is rather weak. When both broken spatial symmetry and broken charge-conjugation symmetry are taken into account, a strong effect on the electronic structure of polyphenylene derivatives is found. In spite of the strong effect of the broken symmetries on the electronic structure, the effect on the optical-absorption spectrum is weak. This surprising result is a consequence of the subtle nature of the configuration interaction in the substituted polyphenylenes within Coulomb-correlated models. We demonstrate numerically an approximate sum rule that governs the strength of an absorption band at 3.7 eV in the absorption spectra of poly(para-phenylene vinylene) (PPV) derivatives. Although substitution can make a previously forbidden transition weakly allowed, the latter acquires strength from a ''finite-size band'' at about the same energy, and not from a higher-energy band at 4.7 eV, as has been previously claimed. It is further predicted that the 3.7-eV band is polarized predominantly along the polymer-chain axis. We have measured the polarization dependence of the optical absorption in an oriented-substituted PPV film. We found that the two lowest-energy absorption bands are polarized predominantly parallel to the chain axis, while the band at 4.7 eV is polarized predominantly perpendicular to the chain axis. These results are in excellent agreement with the theory. [S0163-1829(97)10104-7]

I. INTRODUCTION

In contrast to the polyacetylenes and polydiacetylenes, phenylene-based π-conjugated polymers have multiple-absorption features that extend well into the ultraviolet.[1–3] Recent works by several groups[2–5] have emphasized the importance of fitting the absorption spectra of polyphenylenes over the entire spectral region, within appropriate theoretical models. Such fittings can provide direct information on the role of Coulomb correlations in the polyphenylenes and the excitonic nature of the lowest optical absorption, as well as indirect information on important material parameters like the exciton binding energy, triplet-triplet energy gap, etc. The importance of proper assignment of the different absorptions in the polyphenylene absorption spectra therefore cannot be overstated.

Much of the current discussion is related to early[6–9] as well as more recent[10–12] experimental and theoretical studies of the absorption spectra of cis- and trans-stilbene and related molecules. The qualitative effects of Coulomb interactions on the energies of the relevant excited states, in trans-stilbene in particular, were already understood by the early investigators, and detailed discussions may be found in Ref. 9. At a quantitative level, however, there exist disagreements between very early and more recent work. For example, while the origin of the lowest-energy absorption band in trans-stilbene is agreed upon, the experimentally determined polarizations[11] of the two higher-energy absorption bands in trans-stilbene indicate that the ordering of the relevant energy levels are opposite to that predicted in Ref. 9. In principle, it should still be possible to understand polymeric spectra from the existing literature on trans-stilbene. However, while the absorption spectrum of trans-stilbene contains three dominant bands, polymeric spectra consist of four absorption bands[1–3] (see below), and the bulk of current controversies center around the origin of the additional feature and the resultant implications for the electronic structures and chain lengths of the polymeric materials (see below). It is the goal of this work to understand the origin of this band precisely.

The problem that arises in attempts to understand the experimental absorption spectra of polyphenylenes *vis a vis* theoretical models is that the bulk of the existing experimental data are for the substituted derivatives, rather than for the

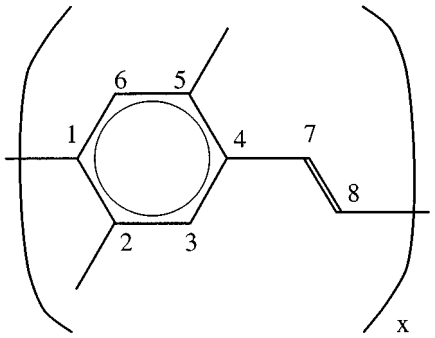

FIG. 1. The unit cell of PPV. Substituent groups are attached to the carbon atoms 2 and 5 in the PPV derivatives. Our numbering scheme of the atoms for the unit cell of PPP is similar, with only the vinylene linkage absent.

unsubstituted materials. In Fig. 1, we show the unit cell of poly(para-phenylenevinylene) (PPV) and our numbering scheme for the carbon atoms. The PPV derivatives which were experimentally investigated have the substituent groups attached to carbon atoms 2 and 5. Meaningful comparisons of theoretical and experimental absorption spectra require that spectral features that are characteristics of the backbone π-electron network are clearly distinguished from those features that result from substitutions. The existing literature on the effect of substitutions is controversial. This is primarily due to the fact that the only unsubstituted polyphenylene whose absorption spectrum as been measured over the entire spectral region of interest is (PPV),[1,2] the lowest absorption feature in which is extremely broad. This may be seen in Fig. 2(a), where the absorption spectrum of PPV is plotted. For comparison, we have shown the absorption spectrum of unoriented poly(2,5-dinonyloxy-1,4-phenylenevinylene) (NO-PPV),[13] where the side groups are OC_9H_{19}, in Fig. 2(b). Four distinct absorption bands, centered at 2.4, 3.7, 4.7, and 6 eV, respectively, are observed in Fig. 2(b). Three out of these four bands are clearly visible in Fig. 2(a), but in the 3.7-eV region only a weak shoulder on the broad lowest-energy absorption is seen. The absorption bands at 2.4, 4.7, and 6 eV are labeled *I*, *III*, and *IV*, respectively, in Figs. 2(a) and 2(b). Whether or not the shoulder at about 3.7 eV in Fig. 2(a) corresponds to a distinct absorption in the unsubstituted PPV is not clear from the experimental spectra alone. Comparison to the absorption spectrum of trans-stilbene[9] suggests that bands *I*, *III*, and *IV* have the same origins as the observed absorption bands in the latter molecule, but the origin of the 3.7-eV feature is not clear from such a comparison.

In the current theoretical literature, the band at 3.7 eV has either been *assumed* to be a characteristic of the π network,[2,3] or it has been ascribed to the broken charge-conjugation symmetry (CCS) in the PPV derivatives.[14] Within the first class of models, the 3.7-eV band should appear in both PPV and its derivatives (note, however, that the wave-function analysis of Ref. 2 implies different origins for this band in PPV and in derivatives). Within the model emphasizing broken CCS, this band is absent in the long chain limit of PPV, but appears in the derivatives with broken CCS.

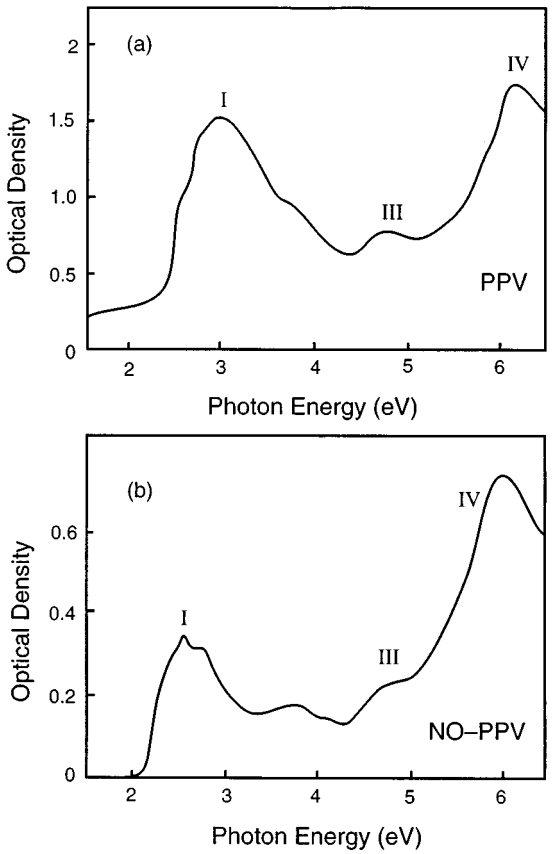

FIG. 2. Absorption spectra of (a) unsubstituted PPV, (b) unoriented NO-PPV. The absorption bands centered at 2.4, 4.7, and 6.0 eV are labeled *I*, *III*, and *IV*, respectively.

The inability of one-electron theory to explain the optical absorption in trans-stilbene has been extensively discussed.[6–9] Similar discussions in the context of the polyphenylenes have been presented by us previously,[3,15] and are also implicit in related theoretical studies.[2,4,5] For the sake of completeness only, we repeat these arguments in Sec. II. In Sec. III, we give a qualitative discussion of the effects of electron-electron interaction on the electronic structure and optical absorption. *We emphasize, however, that our goal in the present paper is not to arrive at the proper magnitudes of the Coulomb correlation parameters that are necessary to describe the phenylene-based polymers;* such quantitative aspects have been discussed elsewhere.[16] In Sec. IV, we present our calculations of substitution effects on the absorption spectra of phenylene-based polymers within the correlated electron model. We establish that within Coulomb-correlated models, *subject to the restriction that transition energies are nearly same in unsubstituted and substituted PPV's,* the effect of broken CCS alone on the electronic structure as well as on optical absorption is tiny. Broken spatial symmetry, on the other hand, has a strong effect on the underlying electronic structure, although the consequence on the absorption spectrum is subtle, due to an approximate sum rule that we demonstrate. In particular, we show that although substitutions can make a previously forbidden optical transition near 3.7 eV weakly allowed, this band has a vanishing intensity in the infinite chain limit of *both* unsubstituted and substituted PPV. Our calculations make specific

predictions for the polarizations of the different absorption bands seen experimentally (see Fig. 2). These predictions have been verified by our experimental effort, as is shown in Sec. V. Finally, in Sec. VI we present our conclusions. One important conclusion that emerges from our work is that the real polymers in all cases consist of relatively short oligomers (8–10 units in chain length). This, in turn, has important implications for the interpretations of transport measurements, as discussed in Sec. VI.

II. INAPPLICABILITY OF BAND THEORY

We write the one-electron Hückel Hamiltonian H_{1e} for unsubstituted PPV as,

$$H_{1e}=-\sum_{\langle ij\rangle,\sigma} t_{ij}[c^{\dagger}_{i,\sigma}c_{j,\sigma}+c^{\dagger}_{j,\sigma}c_{i,\sigma}], \tag{1}$$

where $c^{\dagger}_{i,\sigma}$ creates a π electron of spin σ on carbon atom i, the symbol $\langle ij\rangle$ implies that atoms i and j are nearest neighbors, and t_{ij} is the hopping integral between i and j. In writing Eq. (1) we have neglected the ring rotations in real PPV.[17] The band structure for PPV within Eq. (1) has been discussed in Refs. 3 and 15 (see Fig. 1, Ref. 3). There are four valence (conduction) bands, three of which are delocalized, with nonzero electron densities on all carbon atoms. A fourth localized valence (conduction) band has zero electron densities on the para carbon atoms of the phenyl ring and the two carbon atoms that form the vinylene linkage. We label the delocalized valence and conduction bands as d_j and d^*_j, $j=1-3$, where the numbering scheme is such that d_1 (d^*_1) is the highest (lowest) valence (conduction) band. The localized valence (conduction) band, which occurs in between d_1 and d_2 (d^*_1 and d^*_2), is labeled l (l^*).

The calculated optical absorption for PPV within Eq. (1) (Refs. 3 and 15) consists of three absorption bands in the energy region of interest [see Fig. 1(b) in Ref. 15]. These are (i) an absorption band originating from transitions $d_1\rightarrow d^*_1$, (ii) a central peak due to the degenerate transitions $d_1\rightarrow l^*$ and $l\rightarrow d^*_1$, and (iii) a high-energy peak energy due to the $l\rightarrow l^*$ transitions. An important conclusion of the band model is that the absorption band (ii) is predicted to occur *exactly* at the center between the bands (i) and (iii),[3,4] independent of the chain length. One other result that will turn out to be important later is related to the polarizations of the three types of transitions. Defining the x axis as the line joining the para carbon atoms of PPV, and the y axis as orthogonal to it in the plane of the system, transitions of types (i) and (iii) are calculated to be polarized predominantly along the x axis (with a weak y component), while transition (ii) is polarized predominantly along the y axis (with now a weak x component).[4,14,15]

Although we have discussed PPV in the above, it is to be noted that the band structures of other polyphenylenes are similar. This has also been emphasized by Rice and co-workers.[4] The calculated absorption spectrum of polyparaphenylene (PPP) is similar, with absorption band (ii) once again occurring exactly at the center between bands (i) and (iii). In the case of unsubstituted PPP, absorption bands (i) and (iii) are strictly x polarized, with no y component whatsoever. Similarly, absorption band (ii) is strictly y polarized. We utilize this fact in our calculations in Sec. IV.

The inapplicability of the simple Hückel model becomes obvious from comparing the calculated absorption spectrum with the experimental spectra in Fig. 2. Whether or not the 3.7-eV band appears in the absorption spectrum of Fig. 2(a), the following point remains valid. Neither of the two weak bands in Fig. 2(b), at 3.7 and 4.7 eV, is at the center of the energy scale defined by the two strong absorptions at 2.4 and 6.0 eV, respectively. It is tempting to assign the origin of four absorption bands to substitution-related broken CCS within the *non*interacting electron model of Eq. (1). Within such a model the absorption bands 3.7 and 4.7 eV would be a consequence of the splitting of the central band (ii) due to substitution. The absorption spectrum of *unsubstituted* PPV would then have to be very different, and the 4.7-eV band in PPV would have to be redshifted by about 0.5 eV within this scenario. The occurrence of this feature in PPV at about the same energy as in the derivative proves that such a simplistic approach certainly is not applicable. As we discuss in Sec. III, the considerable shift of the 4.7-eV band from the center finds a natural explanation when electron-electron interactions between the π electrons are included. The argument here is identical to that previously given to explain the absorption spectrum of trans-stilbene.[9] Furthermore, the occurrence of this band at nearly the same energy in PPV and its derivatives indicates that the various transition energies are determined predominantly by the electron-electron interactions, with substitutions playing a weak role. The oscillator strengths of the transitions may or may not be affected by substitutions, and will have to be investigated *within* the Coulomb-correlated model.

III. COULOMB INTERACTION EFFECTS, A QUALITATIVE DISCUSSION

Our theoretical calculations are within a Pariser-Parr-Pople-type Hamiltonian H, written as

$$H=H_{1e}+H_{\rm ee}, \tag{2a}$$

where H_{1e} is the same as in Eq. (1) and $H_{\rm ee}$ is the electron-electron interaction,[18]

$$H_{\rm ee}=U\sum_i n_{i,\uparrow}n_{i,\downarrow}+\tfrac{1}{2}\sum_{i,j} V_{ij}(n_i-1)(n_j-1). \tag{2b}$$

Here $n_{i,\sigma}=c^{\dagger}_{i,\sigma}c_{i,\sigma}$ is the number of electrons with spin σ on site i, $n_i=\Sigma_\sigma n_{i,\sigma}$, and U and V_{ij} are the on-site and intersite Coulomb interactions (note that, unlike t_{ij}, V_{ij} is not restricted to nearest neighbors and is long range).

The qualitative effects of nonzero $H_{\rm ee}$ can be understood from early treatments of electron correlation in the quantum chemistry literature.[7–9,19] The strongest correlation effect is the configuration interaction (CI) between degenerate configurations (first-order CI), which leads to a splitting of the accidental degeneracies characteristic of the Hückel model of Eq. (1). In the present case, the degenerate excitations $d_1\rightarrow l^*$ and $l\rightarrow d^*_1$ are subject to such strong correlation effects.[9] In what follows, we denote singly excited configurations in which an electron has been promoted from the single-particle level i to the single-particle level j as $\chi_{i\rightarrow j}$. Nonzero $H_{\rm ee}$ introduces matrix elements $\langle\chi_{d_1\rightarrow l^*}|H_{\rm ee}|\chi_{l\rightarrow d^*_1}\rangle$, such that nondegenerate eigenstates

(within the simple first-order CI theory) $\chi_{d_1\rightarrow l^*}\pm\chi_{l\rightarrow d_1^*}$ are obtained. For repulsive H_{ee}, states with the ''plus'' combination occur at higher energy, and states with ''minus'' combination are at lower energy.[4,9] Based on this simple picture, one already sees that the theoretical model of Eqs. 2(a) and 2(b) would provide the basis for an explanation of the substantial deviation of the experimental absorption spectra of Figs. 2(a) and 2(b) from the calculated spectrum.

In addition to the energies, dipole selection rules are also of interest. For $H_{ee}=0$, the strengths of the transitions $d_1\rightarrow l^*$ and $l\rightarrow d_1^*$ are exactly equal. Optical transitions to the CI states $\chi_{d_1\rightarrow l^*}-\chi_{l\rightarrow d_1^*}$ are therefore forbidden.[4,9] Thus, although the CI model is able to explain the transition at 4.7 eV in Figs. 2(a) and 2(b), the origin of the peak at 3.7 eV still remains to be explained. This is the goal of the rest of the paper. As we shall show, a number of interesting conclusions emerge in our quest for the proper assignment of this transition.

Before we proceed to Sec. IV, we discuss the parametrization of the Hamiltonian. We use the standard hopping integrals[18–20] $t_{ij}=t_0=2.4$ eV for the phenyl ring, and $t_{ij}=2.2$ (2.6) eV for the single (double) bonds of the vinylene unit in PPV. Our parametrization of H_{ee} is very similar to the Ohno parametrization[21] of the Pariser-Parr-Pople Hamiltonian,

$$V_{ij}=\frac{U}{\kappa(1+0.6117R_{ij}^2)^{1/2}}, \tag{3}$$

where R_{ij} is the distance between atoms i and j in Å, and κ is a parameter that determines the magnitudes of the intersite Coulomb interactions relative to the on-site interaction U. Within the standard Ohno parametrization, $U=11.13$ eV and $\kappa=1$. Unlike the Ohno parametrization, however, we studied many different combinations[16] of U and κ, and showed elsewhere that for $t_0\sim 2.4-2.5$ eV, there exists a single parameter set within Eq. (3), $U=8$ eV and $\kappa=2$, that can fit the locations of all three peaks I, III and IV of Fig. 2 (these values of U and κ can differ if t_0 is taken to be substantially different; however, based on the existing literature,[12,18–20] we believe that the value chosen by us for t_0 is quite reasonable). The slightly smaller U and V_{ij} we require (in comparison to the standard Ohno parameters) may be a reflection of the interchain screening that occurs in the polymeric materials and that is absent in the gas phase molecules. On the other hand, we are forced to choose $\kappa>1$ in order to obtain the correct ordering of the optically allowed excited states. In the case of trans-stilbene, for example, the analysis of Beveridge and Jaffé,[9] based on the bare Coulomb interactions, predicted that the intermediate-energy absorption band was polarized along the long axis of the molecule, while the absorption band at the highest energy was polarized nearly perpendicular to the long axis.[9] This is a consequence of a very large calculated splitting between the $\chi_{d_1\rightarrow l^*}\pm\chi_{l\rightarrow d_1^*}$, so much so that the energy of the ''plus'' combination actually exceeded that of the lowest allowed $l\rightarrow l^*$ state[9] (see Fig. 3 in Ref. 9). The polarization study of the absorption in trans-stilbene in Ref. 11 found that the polarizations of the intermediate and high-energy absorptions are *exactly opposite* to those calculated by Beveridge and Jaffé, indicating a smaller actual energy splitting between the $\chi_{d_1\rightarrow l^*}\pm\chi_{l\rightarrow d_1^*}$. With $\kappa=1$, our calculated results are identical[16] to that of Beveridge and Jaffé. As we show below, the experimental polarizations of bands III and IV in PPV and derivatives are also identical to those of the intermediate- and high-energy absorption bands in trans-stilbene. This latter result could have been anticipated from the relative strengths of experimental bands III and IV in the polymer, and from the band theoretical result that the strength of the $d_1\rightarrow l^*$ and $l\rightarrow d_1^*$ optical transitions, relative to that of the $l\rightarrow l^*$ transition, decreases with chain length. Thus all experimental signatures indicate smaller splittings between $\chi_{d_1\rightarrow l^*}\pm\chi_{l\rightarrow d_1^*}$ than those calculated with the bare interaction parameters. In Ref. 16, we show explicitly that this is best achieved by introducing the screening parameter κ in Eq. (3). In our present work, we report our calculations for the one set of parameters that best reproduce the absolute energies of the four absorption bands. We emphasize that our conclusions regarding substitution effects within Coulomb-correlated models have to do with *symmetry-related effects,* and are not affected by the actual magnitudes of the parameters that enter H_{ee}, although they can affect relative locations of the relevant energy bands.

IV. SUBSTITUTION EFFECTS, NUMERICAL RESULTS

A. Two-unit oligomers

We discuss the effects of electron-electron interactions and chemical substitutions first for the simplest cases, the two-unit oligomers. For the discussion of the substitution effects it is useful to have absorptions polarized strictly along the x and y axes in the parent unsubstituted material. We therefore present the results of detailed calculations for biphenyl (the two-unit oligomer of PPP). The results for trans-stilbene (the two-unit oligomer of PPV) are similar, and are not shown in detail. We emphasize that *the goal of this work is not to explain optical absorption in the real biphenyl[22] or trans-stilbene[8,9,11] molecules,* but to understand the consequences of substitution related broken symmetry. The Coulomb parameters $U=8$ eV and $\kappa=2$ that explain the polymer spectra are slightly too small for the small molecules, whose spectra are explained better if the Ohno parameters are used. This again is probably a consequence of interchain screening in the polymers. The calculations presented here are therefore for *hypothetical* biphenyl and trans-stilbene molecules with smaller Coulomb interactions. Note that this does not alter symmetry effects.

In biphenyl (also in trans-stilbene) the d_1 and d_1^* ''bands'' each consist of a single molecular orbital (MO), whereas the l and l^* ''bands'' each consist of a pair of degenerate MO's. As discussed in Sec. III, there are now four *classes* of eigenstates, labeled as, (i) $\psi_I^{(0)}=\chi_{d_1\rightarrow d_1^*}$, (ii) $\psi_{II}^{(0)}=\chi_{d_1\rightarrow l^*}-\chi_{l\rightarrow d_1^*}$, (iii) $\psi_{III}^{(0)}=\chi_{d_1\rightarrow l^*}+\chi_{l\rightarrow d_1^*}$, and (iv) $\psi_{IV}^{(0)}=\chi_{l\rightarrow l^*}$. Here the superscript ''0'' refers to the unsubstituted molecule. The absorption bands labeled I, III, and IV in Figs. 2(a) and 2(b) correspond to optical transitions to $\psi_I^{(0)}$, $\psi_{III}^{(0)}$, and $\psi_{IV}^{(0)}$, respectively. When necessary, we will distinguish between the wave functions within a given class by adding further subscripts [for example, the two nearly

degenerate wave functions within class (ii) may be distinguished by writing them as $\psi_{IIa}^{(0)}$ and $\psi_{IIb}^{(0)}$, respectively]. Our actual calculations go beyond first-order CI and include *all* single excitations (including those belonging to the outer bands d_1 and d_2^* and d_3 and d_3^*). Thus the true singles CI (SCI) wave functions receive additional weak contributions from configurations involving the outer bands, but can be still *qualitatively* thought of as described above. From the Hückel description, optical excitations from the ground state to $\psi_I^{(0)}$ and $\psi_{IV}^{(0)}$ are x polarized, that to $\psi_{III}^{(0)}$ y polarized, and that to $\psi_{II}^{(0)}$ forbidden.

The substituents in the experimental systems are attached to carbon atoms 2 and 5 of the unit cell shown in Fig. 1. There are two possible effects of substitution on the electronic structure: inductive[23] and mesomeric.[24] The inductive effect is incorporated by including a site-dependent energy term $H_i=\epsilon\Sigma_i c_{i,\sigma}^{\dagger}c_{i,\sigma}$ to the Hamiltonian, where i is a carbon atom directly bonded to a substituent. The mesomeric effect arises from the overlap of the p_z orbital of a carbon atom with the p orbital of a substituent atom containing a lone pair of electrons (in the case of PPV derivatives this is an oxygen atom). It is incorporated by adding $H_m=E_s\Sigma_{s\sigma}c_{s\sigma}^{\dagger}c_{s\sigma}-t_s\Sigma_{is\sigma}(c_{i\sigma}^{\dagger}c_{s\sigma}+c_{s\sigma}^{\dagger}c_{i\sigma})$ to the Hamiltonian,[14] where s refers to the substituent atom directly bonded to the π-skeleton, E_s is its site energy, i is the carbon atom to which the substituent atom is bonded, and t_s is the hopping between these two atoms. The change in the one-electron wave functions due to the two terms are identical in the present case (for the realistic situation $|t_s|\ll|E_s|$; see also Ref. 14), as is easily ascertained by numerically solving $H_{1e}+H_i$ and $H_{1e}+H_m$. The schematic MO energy diagram for substituted biphenyl, excluding the outermost MO's, is shown in Fig. 3(a). The same schematic applies to substituted trans-stilbene. The dashed line in Fig. 3(a) shows the chemical potential, which is closer to the valence band than to the conduction band if the sign of ϵ is reversed. Thus the sign of ϵ in H_i determines the stabilization or destabilization of the single-particle energy levels.[2] It has, however, no effect on energy gaps or optical absorption.

From Fig. 3(a), the main effects of substitution on the MO levels seem to be (a) the breaking of CCS, discussed also in Refs. 2 and 14, and (b) the loss of the twofold degeneracies of the bonding and antibonding localized levels, also discussed in Ref. 2. In the following we refer to the nondegenerate bonding (antibonding) localized levels in the substituted molecules as l_1 and l_2 (l_2^* and l_2^*), the subscript 1 referring to the levels closer to the d_1 and d_1^* MO's. The transitions $d_1\rightarrow l_i^*$ and $l_i\rightarrow d_1^*$ are nondegenerate for nonzero ϵ, and it is tempting to assign the two peaks at 3.7 and 4.7 eV in Fig. 2(b) to these two transitions within the noninteracting electrons model. This would, however, be incorrect, as already pointed out in Sec. II.

There is an additional effect on the MO's upon including H_i or H_m that is not obvious from Fig. 3(a), and that has a stronger effect on the electronic structure for nonzero $H_{\rm ee}$. This is the *loss of localized character* of the MO's l_1, l_2 and l_1^*, l_2^* in Fig. 3(a). This is shown in Fig. 3(b), where we have given the coefficients of the atomic orbitals for the l_1 and l_1^* levels of the substituted biphenyl molecule, calculated numerically for $H_{1e}+H_i$ with $\epsilon=-1$ eV. The effect is similar on the trans-stilbene molecule, as shown in Fig. 3(c)

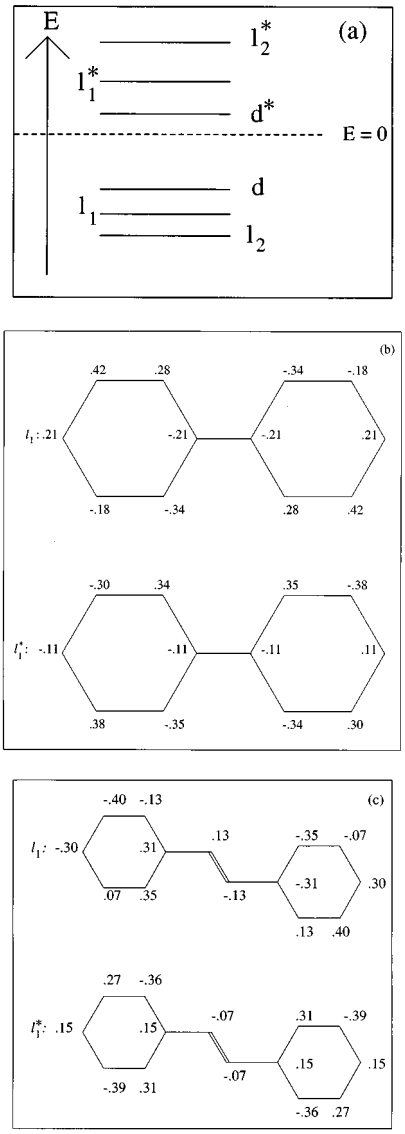

FIG. 3. (a) Schematic MO energy diagram (excluding the outermost MO's) for substituted biphenyl and trans-stilbene. Note the loss of charge conjugation symmetry. The dashed line, indicating the chemical potential, would be closer to the valence-band levels if the sign of ϵ were reversed. (b) Atomic orbital coefficients for the l_1 and l_1^* Hückel MO's of substituted biphenyl with $\epsilon=-1$ eV. Note the loss of localized character. (c) Same as (b) for trans-stilbene.

for the same value of ϵ. The nature of these one-electron wave functions are very similar for nonzero H_m. For simplicity, we therefore discuss the correlated wave functions of the substituted molecules for nonzero H_i only.

In our discussion below, we label the SCI eigenstates of the substituted molecules $\psi_I^{(s)}$, $\psi_{II}^{(s)}$, $\psi_{III}^{(s)}$, and $\psi_{IV}^{(s)}$. Within the broken CCS model,[14] $\psi_{II}^{(s)}$ and $\psi_{III}^{(s)}$ are still linear combinations of $\chi_{d_1\rightarrow l_i^*}$ and $\chi_{l_i\rightarrow d_1^*}$ only, with no contributions from $\chi_{d_1\rightarrow d_1^*}$ or $\chi_{l_i\rightarrow l_i^*}$. The only difference from $\epsilon=0$ (within the broken CCS model) is that the absolute values of the contributions of $\chi_{d_1\rightarrow l_i^*}$ and $\chi_{l_i\rightarrow d_1^*}$ to $\psi_{II}^{(s)}$ are unequal, and therefore their contributions to the overall optical absorption do not cancel. Therefore, if $\psi_{II}^{(s)}$ becomes allowed due to broken CCS, it should be polarized along the y direction,[14] exactly as $\psi_{III}^{(0)}$ and $\psi_{III}^{(s)}$. As already discussed

TABLE I. SCI wave functions and energies of model unsubstituted and substituted biphenyl with $U=8$ eV and $\kappa=2$. The transition dipole moment components (in Å, with electron charge $e=1$) μ_x and μ_y of the excited states with the ground state are also listed, along with the total oscillator strength f of each transition. Note that $f_I^{(0)} \simeq f_I^{(s)} + f_{II}^{(s)}$, where the superscripts ''0'' and ''s'' refer to $\epsilon=0$ and $\epsilon\neq 0$, respectively.

ϵ(eV)	state	Energy (eV)	μ_x	μ_y	f
0.0	ψ_I	4.53	1.12	0.00	5.68
	ψ_{IIa}	4.50	0.0	0.0	0.0
	ψ_{IIb}	4.53	0.0	0.0	0.0
	ψ_{IIIa}	5.45	0.0	0.0	0.0
	ψ_{IIIb}	5.59	0.0	−0.86	4.13
	ψ_{IVa}	6.01	0.104	0.0	0.065
	ψ_{IVb}	6.02	0.0	0.0	0.0
	ψ_{IVc}	6.19	0.0	0.0	0.0
	ψ_{IVd}	6.24	0.918	0.0	5.26
−1.0	ψ_I	4.2	0.884	−0.121	3.34
	ψ_{IIa}	4.2	0.0	0.0	0.0
	ψ_{IIb}	4.77	−0.693	−0.162	2.42
	ψ_{IIIa}	5.29	0.0	0.0	0.0
	ψ_{IIIb}	5.6	−0.061	−0.77	3.34
	ψ_{IVa}	5.9	−0.164	0.301	0.693
	ψ_{IVb}	6.1	0.0	0.0	0.0
	ψ_{IVc}	6.23	0.0	0.0	0.0
	ψ_{IVd}	6.25	0.864	−0.139	4.79

above, the occurrence of the 4.7-eV peak in both unsubstituted PPV and in the substituted derivative implies that the *locations* of the states II and III, though not their oscillator strengths, are determined predominantly by $H_{\rm ee}$, and not by H_i. Below, we examine the oscillator strengths of the transitions to these states with this restriction in mind.

The loss of localized character of the l_i and l_i^* MO's is distinct from the breaking of CCS. The quasidelocalized character of the previously localized levels, when taken together with the broken CCS, has an important effect on the CI wave functions for nonzero $H_{\rm ee}$. Specifically, we show below that for $\epsilon\neq 0$, $\chi_{d_1\rightarrow l_i^*}$ and $\chi_{l_i\rightarrow d_1^*}$ mix with $\chi_{d_1\rightarrow d_1^*}$ and $\chi_{l_i\rightarrow l_i^*}$, and *it is this configuration mixing that contributes predominantly to the oscillator strength of the previously forbidden state.*

In Table I we present the results of SCI calculation of optical absorption in biphenyl for $\epsilon=0$ and -1 eV, respectively. Based on the strong redshift of the lowest-energy optical transition, we conclude that $\epsilon=-1$ eV simulates strong substitution effects. In real fluorine-substituted biphenyls, this shift is considerably smaller.[22] At the same time, the energies of states $\psi_{III}^{(0)}$ and $\psi_{III}^{(s)}$ are close, as required by the experimental results of Figs. 2(a) and 2(b). One of the two $\psi_{II}^{(s)}$ *is* optically allowed, but it is predominantly *x polarized*, in contrast to the prediction of the broken CCS model.[14] Note also that the oscillator strength of the transition to $\psi_I^{(s)}$ is considerably smaller than that to $\psi_I^{(0)}$, indicating that the strongly allowed state I is the origin of the oscillator strength of the previously forbidden state II. Indeed, from the oscillator strengths of these states in Table I, one can discern the existence of an approximate sum rule that governs the overall strength of transitions I and II, viz. $f_I^{(0)} \simeq f_I^{(s)} + f_{II}^{(s)}$. Although there is a small decrease in the oscillator strength of the transition to state III, this is accompanied by the appearance of a weak y component in the transition to state IV, indicating a redistribution of dipole moments between states III and IV. Because of the greater contributions by the outer bands in these higher-energy states, there is a stronger deviation from a precise sum rule in this energy range. Any mixing between states II and III would be reflected in the strength of the dipole coupling of $\psi_{II}^{(s)}$ in the y direction; *the very small magnitude of this indicates that broken* CCS *by itself plays a weak role in the absorption spectra of the substituted molecules.*

Further understanding of the effect of substitution comes from the examination of the CI wave functions. Detailed analysis of these data can be found elsewhere (see Table II of Ref. 15). Here we only present our conclusions. In the unsubstituted biphenyl, the forbidden (allowed) character of $\psi_{II}^{(0)}$ ($\psi_{III}^{(0)}$) is reflected in the opposite (same) signs of the contributions by $\chi_{d_1\rightarrow l_i^*}$ and $\chi_{l_i\rightarrow d_1^*}$ to the y component of the dipole coupling to the ground state. In the substituted case, the magnitudes of the contributions of $\chi_{d_1\rightarrow l_i^*}$ and $\chi_{l_i^*\rightarrow d_1^*}$ to $\psi_{II}^{(s)}$ *are* different, but the signs of these contributions remain opposite. The difference in the magnitudes are simply too small to make an observable contribution to the y component of the dipole moment of this state.[15] The bulk of the dipole coupling of $\psi_{II}^{(s)}$ to the ground state actually comes from the $\chi_{d_1\rightarrow d_1^*}$ component of the wave function, followed by weaker contributions along the x direction by $\chi_{l_i\rightarrow l_i^*}$ and $\chi_{d_1\rightarrow l_2^*}$ (the latter acquires some x character upon substitution). The strong contribution from $\chi_{d_1\rightarrow d_1^*}$ explains the x polarization of the absorption to this state in Table I. A similar effect leads to the redistribution of oscillator strength between states $\psi_{III}^{(s)}$ and $\psi_{IV}^{(s)}$, which are superpositions of $\psi_{III}^{(0)}$ and $\psi_{IV}^{(0)}$.

The calculated absorption spectra for the two cases, the hypothetical unsubstituted and substituted biphenyl molecules, are shown in Fig. 4, where we have also given the polarizations of the various absorption bands. It is clear from Fig. 4 that the appearance of band II for $\epsilon=-1$ eV is accompanied by a huge reduction in the strength of band I. The very strong effect on the oscillator strength of band I indicates again that unusually large substitution effects are simulated by $\epsilon=-1$ eV. The redistribution of the oscillator strengths between bands III and IV upon substitution is also obvious. The results of our calculations for trans-stilbene are very similar. We conclude that the absorption spectra of the substituted and unsubstituted two-unit oligomers can in principle be different, and a previously forbidden transition can become allowed in the substituted molecules. However, this transition acquires an oscillator strength from the strongly allowed band I of the substituted molecule and not from band III, as has been predicted within the broken CCS model.[14]

B. Four-unit oligomers

In longer chains a phenomenon occurs that is absent in the dimer. This can be anticipated from the Hückel MO energy

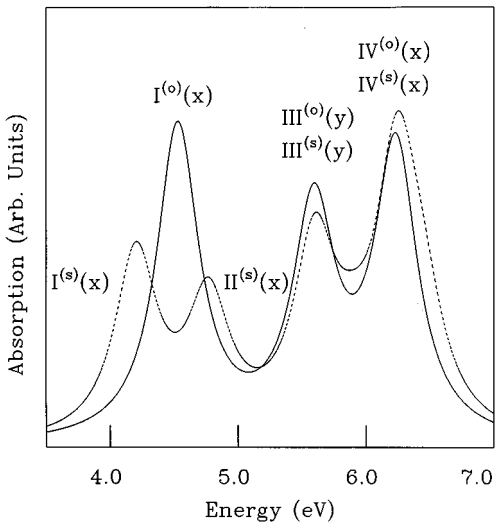

FIG. 4. Calculated absorption spectra of unsubstituted (solid curve) and substituted (dashed curve) biphenyl. States I–IV and the superscripts ''0'' and ''s'' are defined in the text, and the ''x'' and ''y'' in parentheses denote the polarizations of the absorption bands. The absorption band $II^{(s)}$ in the substituted molecule is clearly seen to appear at the expense of absorption band $I^{(0)}$.

diagrams (see Fig. 1, Ref. 3). The d_1 and d_1^* ''bands'' now contain multiple MO's, with discrete energy gaps between them in finite oligomers. In the four-unit PPV oligomers, for example, there are three such MO's in the d_1 and d_1^* bands (the l and l^* ''bands'' are each quadruply degenerate). Multiple $d_1 \rightarrow d_1^*$ transitions are possible now at the Hückel limit, and for nonzero H_{ee} CI occurs between the different $\chi_{d_1 \rightarrow d_1^*}$ in the unsubstituted oligomer. As a consequence, more than three absorption peaks occur for nonzero H_{ee} even in the unsubstituted oligomer (for $H_{ee}=0$, the energy separations between the discrete states are considerably smaller, and the band result is reached faster[2–4]). Figure 5 shows the absorption spectrum of a four-unit oligomer of unsubstituted PPV, calculated with our H_{ee} parameters. The peaks labeled I, III, and IV in Fig. 5 have the same characters as in the dimer, i.e., they originate from transitions to states belonging to the classes $\psi_I^{(0)}$, $\psi_{III}^{(0)}$, and $\psi_{IV}^{(0)}$, whereas the peak labeled Ib arises from transition to a state whose CI wave

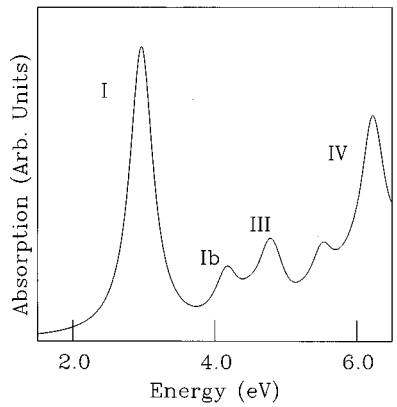

FIG. 5. Calculated absorption of a four-unit oligomer of PPV. The labels on the peaks are described in the text.

TABLE II. Same as Table I for the four-unit oligomer. Note that $f_{Ib}^{(0)} \simeq f_{Ib}^{(s)} + f_{II}^{(s)}$. Only two of the four $\psi_{II}^{(s)}$ are allowed upon substitution. The other two mix with the $\chi_{d_1 \rightarrow d_1^*}$ of A_g symmetry, and remain forbidden. These forbidden states are not shown for the case of $\epsilon=-1$ eV. The states of the types ψ_{III} and ψ_{IV} are not relevant to our discussion.

ϵ (eV)	state	Energy (eV)	μ_x	μ_y	f
0.0	ψ_I	2.93	2.16	−0.579	14.5
	ψ_{Ib}	4.15	−0.754	0.192	2.51
		4.45	0.361	−0.0813	0.609
	ψ_{II}	4.0	0.0	0.0	0.0
		4.0	0.0	0.0	0.0
		4.23	0.0	0.0	0.0
		4.23	0.0	0.0	0.0
−1.0	ψ_I	2.87	2.16	−0.605	14.4
	ψ_{Ib}	4.02	−0.452	0.307	1.20
		4.11	0.181	∼0	0.135
		4.42	−0.274	0.0736	0.356
	ψ_{II}	3.95	−0.379	−0.0556	0.58
		4.26	−0.514	−0.0357	1.13

function has dominant contributions from higher $\chi_{d_1 \rightarrow d_1^*}$, and weak contributions from the lowest $\chi_{d_1 \rightarrow d_1^*}$ (i.e., the relative weights are different from that of $\psi_I^{(0)}$). Peak Ib gradually merges with peak I in the very long chain limit (greater than 16 units in our calculations) of the unsubstituted material.[4,16] This then leads to two possible origins of the 3.7-eV band in Fig. 2: the finite-size effect and substitution effect. In Ref. 14, broken CCS due to substitution was ascribed as the origin of this transition. In view of our results for the two-unit molecule, this conclusion already looks doubtful. Below, we examine the case of the correlated four-unit molecules, which exhibit all the complexities of longer chains. As seen below, a number of interesting conclusions emerge.

As with the two-unit molecules, we have done full SCI calculations for the unsubstituted as well as substituted four-unit PPV oligomer. The dominant effect of nonzero H_i is once again the quasi delocalized nature of the nominally localized Hückel MO's in the substituted oligomer [see Figs. 3(b) and 3(c)], leading to extensive CI between the $\chi_{d_1 \rightarrow d_1^*}$, $\chi_{d_1 \rightarrow l^*}$ and $\chi_{l \rightarrow \chi_{d_1 \rightarrow ^*}}$, and $\chi_{l \rightarrow l^*}$ for nonzero H_{ee}. The only difference from the two-unit molecules is that in the longer oligomers the forbidden band is expected to acquire oscillator strength at the expense of the finite-size band Ib in Fig. 5, rather than from the strong lowest-energy band I, which is now further away in energy. Note that the states $\psi_{Ib}^{(0)}$ and $\psi_{II}^{(0)}$ have been found to be very close in energy also in previous calculations.[2–4]

The above conjectures are verified from analyses of the calculated absorption and wave functions. As shown in the case of the two-unit oligomer, the polarizations of the calculated absorptions are distinct signatures of the dominant broken symmetry effect. In Table II we present the x and y components of the dipole moments of ψ_I, ψ_{Ib}, and ψ_{II} for the unsubstituted and substituted four-unit PPV oligomer as well as the total oscillator strengths. There is considerable

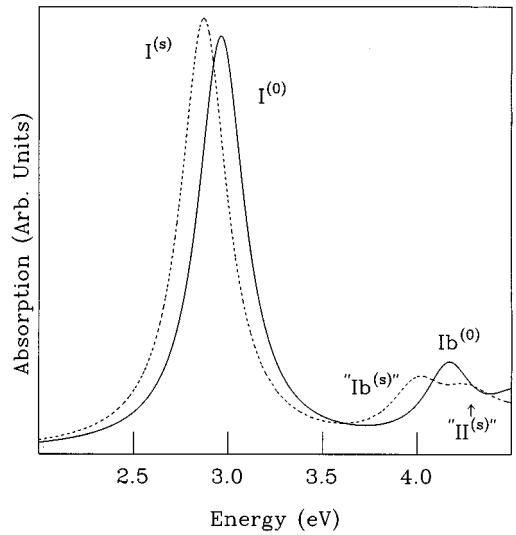

FIG. 6. The low-energy region of the calculated absorption of unsubstituted (solid curve) and substituted (dashed curve) four-unit oligomers of PPV. In the 4.0–4.5-eV region, note the increase in the absorption upon substitution at lower energies, predominantly due to a redshift of $Ib^{(s)}$, and the decrease at higher energies where oscillator strength has been transferred to $II^{(s)}$. The quotation marks around the peak labels indicate only the dominant contribution of the relevant wave functions (see Table II). The nearly constant oscillator strength in this region both before and after substitution indicates that the previously forbidden absorption is becoming allowed at the expense of the ''finite-size band'' (see also Table II).

mixing between states of the types Ib and II upon substitution. Nevertheless, the classification of states as $\psi_{Ib}^{(s)}$ and $\psi_{II}^{(s)}$ is still possible through examination of the dominant components of the wave functions. Exactly as in Table I, the forbidden peak II is allowed in the substituted material, but is strongly x polarized. From the changes in the oscillator strengths of the states Ib and II upon substitution, it is clear that the oscillator strength of II is being borrowed from peak Ib. Note that now $f_I^{(0)} \simeq f_I^{(s)}$ (i.e., the strength of the transition to the lowest state is now unaffected, unlike the two-unit case), but $f_{Ib}^{(0)} \simeq f_{Ib}^{(s)} + f_{II}^{(s)}$. We have made a detailed analysis of the contributions to the overall dipole moments of the various classes of eigenstates by the individual $\chi_{j\to k}$. As in the two-unit case, this analysis merely confirms our interpretation of the calculated polarizations of the different absorptions. In the four-unit oligomer, the redistribution of oscillator strengths between states III and IV is considerably more complicated because of the overlaps in energies of the highest III-type states and the lowest IV-type states. This is, however, not relevant to our discussion: the polarizations of the peaks in the energy region of Ib and II, as well as the sum rule, clearly indicates the strong mixing of the states Ib and II. This is explicitly shown in Fig. 6, where we have plotted the absorption spectra of the unsubstituted and substituted four-unit molecules in the low photon energy region. The absorption band near 4 eV in the substituted molecule has broadened considerably, which is a signature of contributions from both $\psi_{Ib}^{(s)}$ and $\psi_{II}^{(s)}$. The oscillator strength of this band in the low-energy region increases, while the oscillator strength in the high-energy region decreases, such that the overall oscillator strength of the band remains roughly the same.

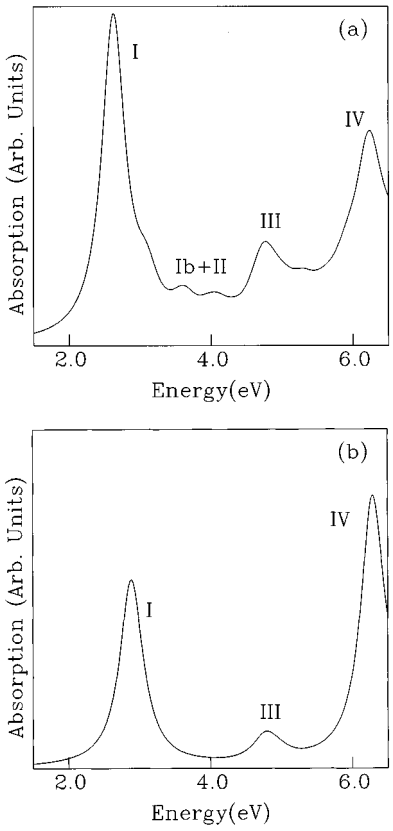

FIG. 7. (a) Calculated absorption spectrum of an eight-unit oligomer of substituted PPV ($\epsilon=-1$ eV). Note the nearly quantitative fits of all absorption bands with the experimental spectra of Figs. 2(a) and 2(b). (b) Calculated absorption spectrum of the same substituted oligomer with all finite-size effects eliminated. Only one Hartree-Fock MO has been retained in both the d_1 and d_1^* ''bands'' at the SCI stage of the calculation here (see text). Note that the second absorption band due to $Ib^{(s)}$ and $II^{(s)}$ has completely disappeared.

C. Longer oligomers

We have done similar calculations for even longer oligomers, and in all cases the results are the same as in the four-unit case. The analyses quickly become highly involved, however, We therefore demonstrate our result using a different approach. In Fig. 7(a) we show the absorption spectrum for an eight-unit substituted PPV oligomer ($\epsilon=-1$ eV). The calculated spectrum is now remarkably similar to the experimental spectrum of Fig. 2(b), with nearly quantitative fitting even to the experimental absorption energies (this fitting is the basis of our choice of the particular Coulomb parameters used here[16]). We now repeat the eight-unit $\epsilon=-1$ eV calculation with only one modification. The Hartree-Fock calculation that precedes the SCI calculation is done for the complete set of MO's. At the SCI step, however, we discard all d_1 MO's except the highest occupied MO, and all d_1^* MO's except the lowest unoccupied MO. This procedure eliminates the possibility of having any absorption due to finite-size effects, but the extent to which a forbidden transition of the type II becomes allowed due to broken CCS remains unchanged. The weak second absorption band seen in Fig. 7(a) at about 3.8 eV is completely absent in Fig. 7(b), indicating clearly its ''finite-size'' origin in the former case.

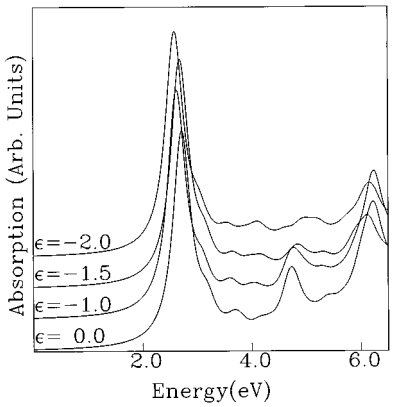

FIG. 8. Calculated absorption spectra of the eight-unit PPV oligomer with several different ϵ. The strong blueshift of band *III* for $\epsilon=-1.5$ and -2 eV by as much as 0.4 eV indicates that these values for ϵ are unrealistically large [see Figs. 2(a) and 2(b)].

D. MAGNITUDE OF ϵ

Our calculations in the previous subsections are for $\epsilon=-1$ eV, based on our reasoning that this value of ϵ already simulates very large substitution effects, as seen from Fig. 4. We show here that this conclusion remains unaltered even for long oligomers. In Fig. 8 we have shown the calculated absorption spectra for the eight-unit oligomer with $\epsilon=0$, -1 eV, -1.5 eV, and -2 eV, respectively. Note that the location of the band *III* for $|\epsilon|\leqslant 1$ eV in Fig. 8 is practically the same as the 4.7-eV band in the experimental spectra of Figs. 2(a) and 2(b). The latter conclusion remains unaltered even when we examine the absorption spectra of other substituted PPV derivatives.[2,3] The shift of band *III* in Fig. 8, however, is very large for $\epsilon=-1.5$ and -2 eV. For $\epsilon=-2$ eV in particular, this shift is about 0.4 eV. We therefore conclude that although $|\epsilon|$ larger than 1 eV can in principle increase the effect of broken CCS in our calculations, such values are unrealistic.

From the above results then, we conclude that in the two-unit molecules as well as in longer oligomers the forbidden state ψ_{II} mixes with states that have predominantly $\chi_{d_1\rightarrow d_1^*}$ character. The two-unit oligomer is a special case only because of the absence of the ''finite-size band,'' which requires multiple MO's in the d_1 and d_1^* bands. In the longer oligomers, absorption band *II* becomes allowed upon substitution at the expense of band *Ib*, and the overall absorption spectrum does not change. *Therefore for band II to appear in the substituted oligomer, band Ib must preexist in the unsubstituted molecule.* This leads us to the following conclusions: (i) the 3.7-eV band in the so-called polymeric materials is a distinct signature of finite chain lengths, and (ii) this particular band is predominantly *x* polarized. In Sec. V, we verify prediction (ii) experimentally.

V. EXPERIMENTAL RESULTS

We have measured the polarized absorption of an oriented thin film of NO-PPV, where the side groups are OC_9H_{19}. A thin film of this polymer was spin coated from 0.7 wt % chloroform solution onto a quartz glass substrate. After evacuation for 2 h at room temperature to eliminate the residual solvent, the film was subjected to a unidirectional rubbing treatment with rayon cloth.[25] The NO-PPV chains were then mostly oriented as deduced from measuring the polarized photoluminescence, which showed a polarization ratio $I_\parallel/I_\perp=5$, where $I_\parallel$ and $I_\perp$ are the photoluminescence intensities parallel and perpendicular, respectively, to the chain directions. We note that these films do not contain polyethylene as in other oriented PPV films described in the literature,[26] and therefore the absorption spectrum does not contain any absorption bands or polarization properties due to the host material.

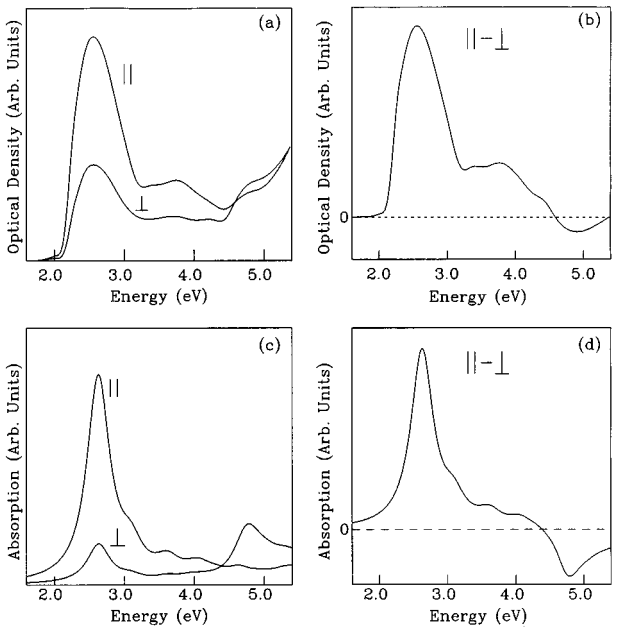

FIG. 9. (a) Experimental optical densities (OD's) parallel and perpendicular to the chain axis of oriented NO-PPV. (b) The measured difference OD, obtained by subtracting the perpendicular OD from the parallel OD in (a). (c) The calculated absorption for a eight-unit substituted PPV oligomer, parallel and perpendicular to the chain axis. (d) The calculated difference spectrum, obtained by subtracting the perpendicular absorption from the parallel absorption of (c).

The polarized absorption was measured using a Perkin-Elmer λ-9 commercial spectrometer, with a resolution of 0.3 nm, which was modified by inserting a polarization scrambler and a Glen-Thompson broadband polarizer assembly (Special Optics). The polarization scrambler was used to avoid extra polarization by the dispersion element inside the spectrometer. The spectrum range of the polarized absorption set up was 1.5–5.5 eV (Glen-Thompson polarizers are very trustworthy up to 5 eV, but in the 5–6-eV range they gradually become less effective). The direction of the polarized light was chosen to be parallel or perpendicular to the NO-PPV chain orientation.

Figure 9(a) shows the polarized optical density (OD) of the oriented NO-PPV film. As is clearly seen, only band *III*, centered at 4.7 eV, has a substantial strength in the perpendicular configuration (perpendicular to the chain direction). Band *I* does have a weak perpendicular component, but this is expected for PPV (see Table II). Similarly the band at 3.7 eV is also mostly polarized in the parallel direction. We also observe that band *III* makes a minor contribution in the parallel direction, which is expected in the case of substituted

PPV within our calculations due to mixing with the high-energy band at 6 eV (see Table I). A better presentation of the polarized absorption is obtained when the optical density in the perpendicular direction is subtracted from the optical density in the parallel direction to eliminate the OD of most of the unoriented chains, which contribute equally in parallel and perpendicular polarized absorption. In Fig. 9(b) we have also included a plot of the difference spectrum $OD_{\parallel}-OD_{\perp}$. This plot shows quite clearly that the bands *I* and *II* are strongly polarized along the axis of the oriented chains, whereas band *III* is polarized mostly perpendicular to the chain axis.

In Fig. 9(c) we show the calculated absorptions in the directions parallel and perpendicular to the chain axis of an eight-unit PPV oligomers, while Fig. 9(d) shows the plot of the calculated difference spectrum (parallel minus perpendicular spectrum). The experimental spectra are in excellent agreement with the calculated spectra, thus confirming the theoretical analysis of Sec. IV. The larger widths of the experimental absorption bands are due to phonon replica, which have not been included in the calculation. This, however, is not a problem, as the 3.7-eV absorption feature is too far removed in energy from absorption band *I* to be a phonon sideband.

VI. CONCLUSIONS

In summary, within the Coulomb-correlated theoretical model for the phenylene-based conjugated polymers, the absorption spectra of the unsubstituted and substituted materials (with the same chain lengths) are expected to be practically identical. Thus for the 3.7-eV band to appear in the substituted PPV, this band had to preexist in the unsubstituted material with the same chain length. In the infinite chain limit, we do not expect a separate 3.7-eV band in either the unsubstituted polymer or its substituted derivative. Our calculations indicate that the absorption bands centered at 2.4, 3.7, and 6 eV are polarized predominantly along the chain axis, while the absorption band centered at about 4.7 eV is polarized predominantly perpendicularly to the chain. The measured polarizations of the absorption bands in very carefully prepared oriented samples of NO-PPV are in excellent agreement with our calculations.

As already mentioned above, the appearance of the 3.7-eV band in the experimental absorption spectra indicates that in all cases the real polymers consist of short chains. Based on the relative strength of the 3.7-eV band, we would guess that the majority of the chains in the experimental samples are 8–10 units in length. This has important implications for the transport behavior. From our calculations, the exciton energy, as well as the energy of the state that constitutes the threshold of the conduction band, have practically converged to their infinite chain values at these chain lengths. The exciton binding energy is defined traditionally to be the difference between the energy of the conduction-band threshold and that of the exciton, and it is this quantity that has been calculated to be 0.9 ± 0.15 eV in our previous work.[3] The calculation energy gaps between the eigenstates above the conduction-band threshold state are, however, still 1–3 kT in chains of length 8–10 units. Thus a true continuum is not reached in the experimental polymers, and it is conceivable that the photoconductivity receives strong contributions from various interchain exciton dissociation processes. Thus the quantity referred to as the ''exciton binding energy'' in photoconductivity experiments may be quite different from the traditional binding energy. This may partially explain the controversies in this area. On the other hand, we have ascribed picosecond photoinduced absorption in these systems to the optical transition from the exciton to a biexciton state of even parity.[27,28] The energy E_{BX} of the one-dimensional biexciton obeys the relationship $E_{\mathrm{BX}}>2\times E_X$ −B.E., where E_X is the exciton energy and B.E. the binding energy of the exciton, *defined in the traditional manner.* Similarly, an even-parity state at 2.9 eV, that is forbidden in linear absorption and that becomes visible in electroabsorption,[27] is a higher-energy charge-transfer exciton that occurs below the continuum threshold. The location of this state is also a measure of the lower limit of the exciton binding energy, again defined traditionally. Thus the calculated B.E. is a relevant physical quantity for all intrachain photophysical measurements, even in the short chains that constitute the real polymers.

ACKNOWLEDGMENTS

We thank V. Massardier for the unsubstituted PPV films. Work at Arizona was supported by the National Science Foundation (NSF) (Grant No. ECS-9408810), the Air Force Office of Scientific Research (Contract No. F49620-93-1-0199), and the Office of Naval Research (Grant No. N00014-94-1-0322). Work at Utah was supported by the U.S. Department of Energy DOE (Grant No. DE-FG-03-93.ER 45490) and the ONR (Grant No. N00014-94-1-0853).

*Present address: NCCOSC, RDT&E division, Code D364, San Diego, CA 92152.

[1] D. A. Halliday, P. L. Burn, R. H. Friend, D. D. C. Bradley, A. B. Holmes, and A. Kraft, Synth. Metals **55-57**, 954 (1993).

[2] J. Cornil, D. Beljonne, R. H. Friend, and J. L. Brédas, Chem. Phys. Lett. **223**, 82 (1994).

[3] M. Chandross, S. Mazumdar, S. Jeglinski, X. Wei, Z. V. Vardeny, E. W. Kwock, and T. M. Miller, Phys. Rev. B **50**, 14 702 (1994).

[4] M. J. Rice and Yu. N. Gartstein, Phys. Rev. Lett. **73**, 2504 (1994); Yu. N. Gartstein, M. J. Rice, and E. M. Conwell, Phys. Rev. B **52**, 1683 (1995).

[5] Y. Shimoi and S. Abe, Synth. Metals (to be published).

[6] J. Dale, Acta Chem. Scand **11**, 971 (1957).

[7] H. H. Jaffé, S. J. Yeh, and R. W. Gardener, J. Mol. Spectrosc. **2**, 120 (1958).

[8] H. Suzuki, Bull. Chem. Soc. Jpn. **33**, 379 (1960).

[9] D. L. Beveridge and H. H. Jaffé, J. Am. Chem. Soc. **87**, 5340 (1965).

[10] G. Orlandi, P. Palmieri, and G. Poggi, J. Am. Chem. Soc. **101**, 3492 (1979).

[11] G. Hohlneicher and B. Dick, J. Photochem. **27**, 215 (1984).

[12] Z. G. Soos, S. Ramasesha, D. S. Galvão, and S. Etemad, Phys. Rev. B **47**, 1742 (1993).

[13] M. Hamaguchi and K. Yoshino, Jpn. J. Appl. Phys. **33**, L1478 (1994); **33**, L1689 (1994).

[14] Yu. N. Gartstein, M. J. Rice, and E. M. Conwell, Phys. Rev. B **51**, 5546 (1995).
[15] S. Mazumdar and M. Chandross, Proc. SPIE **2528**, 62 (1995).
[16] M. Chandross and S. Mazumdar, following paper, Phys. Rev. B **55**, 1497 (1997).
[17] D. Chen, M. J. Winokur, M. A. Masse, and F. E. Karasz, Polymer **33**, 3116 (1992).
[18] D. Baeriswyl, D. K. Campbell, and S. Mazumdar, in *Conjugated Conducting Polymers*, edited by H. Kiess (Springer-Verlag, Heidelberg, 1992), pp. 7–133.
[19] L. Salem, *The Molecular Orbital Theory of Conjugated Systems* (Benjamin, New York, 1966), pp. 408–435.
[20] A. J. Heeger, S. Kivelson, J. R. Schrieffer, and W.-P. Su, Rev. Mod. Phys. **60**, 781, 1988.
[21] K. Ohno, Theor. Chim. Acta **2**, 219 (1964).
[22] T. G. McLaughlin and L. B. Clark, Chem. Phys. **31**, 11 (1978).
[23] J. N. Murrell and H. C. Longuet-Higgins, Proc. Phys. Soc. London Sect. A **68**, 329 (1955).
[24] J. N. Murrell, Proc. Phys. Soc. London Sect. A **68**, 969 (1955).
[25] M. Hamaguchi and K. Yoshino, Jpn. J. Appl. Phys. **34**, L712 (1995).
[26] T. W. Hagler, K. Pakbaz, K. F. Voss, and A. J. Heeger, Phys. Rev. B **44**, 8652 (1991).
[27] J. M. Leng, S. Jeglinski, X. Wei, R. E. Benner, Z. V. Vardeny, F. Guo, and S. Mazumdar, Phys. Rev. Lett. **72**, 156 (1994); Mol. Cryst. Liq. Cryst. **256**, 1 (1994).
[28] F. Guo, M. Chandross, and S. Mazumdar, Phys. Rev. Lett. **74**, 2086 (1995).